

## Supporting Information

# Radical Anion Formation Exhibiting “Turn-on” Fluorescence Sensing of Hydrazine Using a Naphthalene Diimide (NDI) Derivative of Donor-Acceptor-Donor (D-A-D) Molecular Structure

P.Lasitha <sup>\*a,b</sup>

<sup>a</sup>Department of Chemistry, Indian Institute of Technology-Madras, Chennai, 600036, India

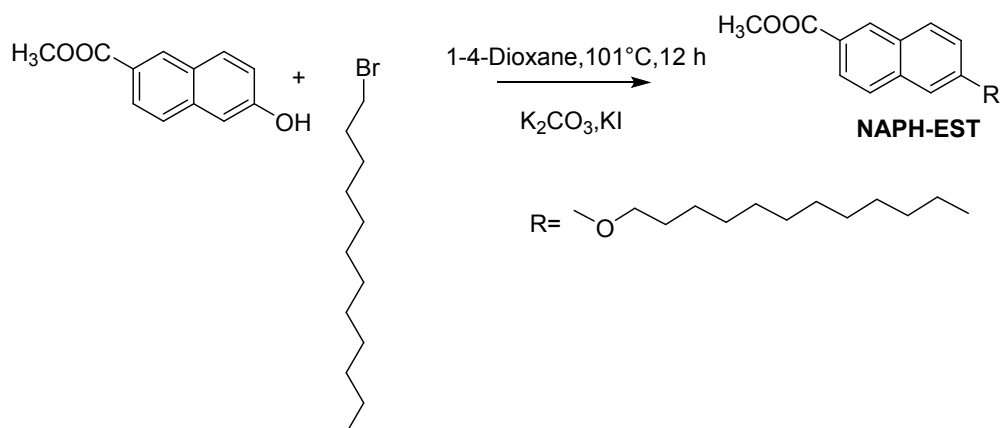
<sup>b</sup>(current affiliation) Department of Chemistry, Indian Institute of Technology -Bombay, 400076,  
Mumbai, India

---

<b>Table of contents</b>	
The synthetic procedure of the compounds	Page 2-4
Quantum yield calculation, the kinetics of self-assembly equations and gelation procedure	Page 4-6
<b>Figure S1-S17</b> , TGA, DSC, OPM, SEM, and spectroscopic studies	Page 7-15
<b>Figure S18-S23</b> , NMR and mass spectra of compounds	Page 15-20

## Synthetic procedure for the compounds

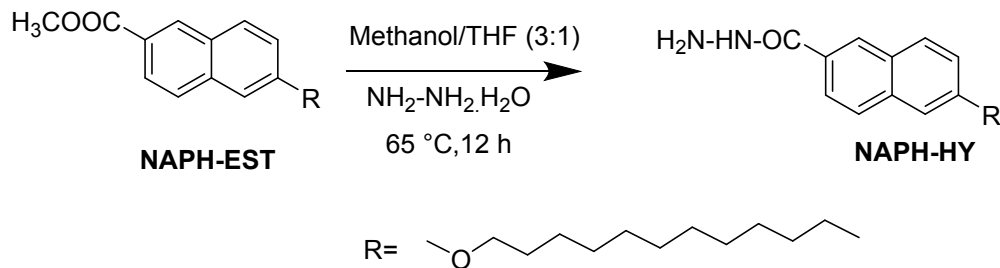
### Synthesis of NAPH-EST



### Scheme S1: Synthesis of NAPH-EST

6-hydroxy-2-naphthoate (1 g, 0.0049 mole), potassium carbonate (1.36 g, 0.0098 mole) and 30 mL 1,4-dioxane were taken in a 250 mL round bottom flask. 1-bromododecane (1.83 g, 0.007 mole) was added to the mixture followed by the addition of a catalytic amount of tertiary butyl ammonium iodide (0.05 g, 0.0003 mole). The reaction mixture was then refluxed for 24 hours, allowed to cool to room temperature. The solvent was evaporated and extracted with ethyl acetate-water mixture. The organic layer was dried over anhydrous  $Na_2SO_4$ , crystallized from methanol to get compound NAPH-EST (1.6 g, 88 % yield).  $^1H$  NMR (500 MHz,  $CDCl_3$ ) : $\delta$ , ppm 0.86 (t, 3H), 1.48 (m, 16H), 1.80 (t, 2H), 1.84 (t, 2H), 3.9 (s, 3H), 4.0 (d, 2H), 7.1 (d, 1H), 7.81 (d, 1H), 7.9 (d, 1H), 8.4 (d, 1H).  $^{13}C$  NMR (100 MHz,  $CDCl_3$ ) : $\delta$ , ppm: 14.2, 22.8, 26.2, 29.3, 29.5, 29.8, 32.08, 52.2, 68.3, 106.5, 120.0, 125.2, 126.0, 126.9, 127.9, 130.9, 130.98, 131.0, 131.03, 137.38, 159.27, 167.59. IR (KBr)  $\nu$ ,  $cm^{-1}$  = 2917, 2848, 1713, 1635, 1611, 1506, 1484, 1466, 1452, 1327, 1389, 1349, 1317, 1297, 1269, 1235, 1183, 1118, 1064. ESI-MS: m/z Calcd for  $C_{24}H_{34}O_3$ : 370.52, found: 409.21[M+K] $^+$ .

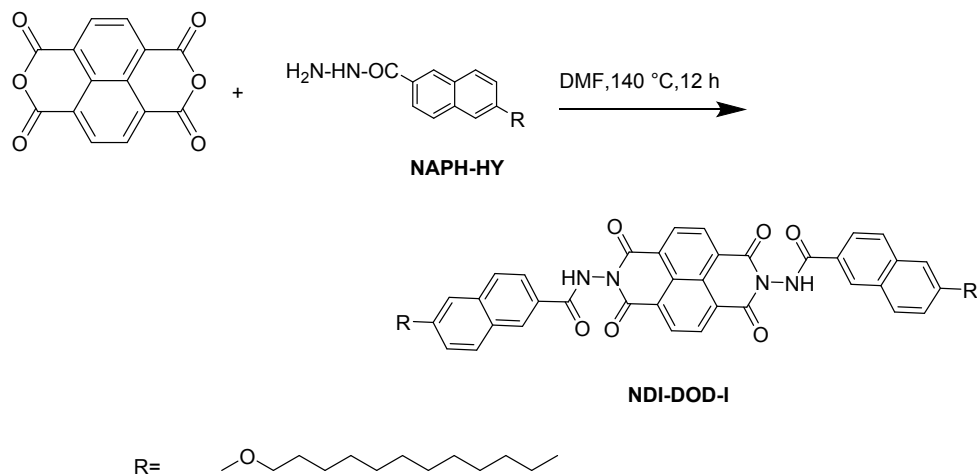
## Synthesis of NAPH-HY



### Scheme S2: Synthesis of NAPH-HY

NAPH-EST (1 g, 0.0026 mole) and hydrazine monohydrate (6.3 mL, 0.13 mole) were dissolved in MeOH /THF (30 mL/15mL) and stirred at  $60^\circ\text{C}$  for 12 hours. The reaction mixture was cooled to room temperature; solvent was evaporated by applying vacuum. The residue was dissolved in DCM and washed many times with water to remove excess of hydrazine mono hydrate. The organic layer was then dried over anhydrous  $\text{Na}_2\text{SO}_4$ . Crude product was purified by column chromatography ethyl acetate /Hexane (3:7) mixture as eluent to obtain NAPH-HY (0.8g, 83 % yield);  $^1\text{H NMR}$  (500 MHz,  $\text{CDCl}_3$ ) : $\delta$ , ppm 0.85 (t, 3H), 1.24(m,16H), 1.47 (q, 2H),1.83 (q, 2H), 2.38 (s,1H), 4.05 (t, 2H), 7.1-7.18(m, 2H), 7.7-7.78 (m, 3H),8.18 (s,1H).  $^{13}\text{C NMR}$  (100 MHz, $\text{CDCl}_3$ ) : $\delta$ , ppm 14.1, 22.6, 26.07, 29.3, 29.6, 31.9, 68.1, 106.3, 120.1, 123.6, 127.2, 127.3, 12.8, 130.4, 136.5, 158.7, 168.88. IR (KBr)  $\nu$ ,  $\text{cm}^{-1}$  = 3283, 3243, 3049, 2954, 2924, 2854, 1650, 1620, 1592, 1507, 1471, 1387, 1365, 1343, 1264, 1220, 1176, 1124, 1100, 1019 1. ESI-MS: m/z Calcd for  $\text{C}_{23}\text{H}_{34}\text{N}_2\text{O}_2$ : 370.53, found: 371.26  $[\text{M}+\text{H}]^+$ .

## Synthesis of NDI-DOD-I



### Scheme S3: Synthesis of NDI-DOD-I

Naphthalene dianhydride (1 g, 0.0037 moles) and **NAPH-HY** (3.4 g, 0.0092 moles) were taken in 30 mL of dry DMF and were heated to 140 °C for 12 hours. The reaction mixture was allowed to cool down to room temperature, extracted with DCM, and washed many times with water. The organic layer was dried over anhydrous  $\text{Na}_2\text{SO}_4$ . The crude product was then purified by column chromatography methanol / $\text{CHCl}_3$  (1:9) mixture as eluent to obtain a brown coloured powder (2.8 g, 80% yield).  **$^1\text{H NMR}$  (500 MHz,  $\text{DMSO-d}_6$ , at 120 °C):**  $\delta$ , ppm 0.88 (t, 8H), 1.5 (s, 5H), 1.87 (s, 4H), 4.1 (t, 4H), 8.4 (s, 4H), 8.3 (m, 3H), 7.7-7.87 (m, 6H), 7.1-7.22 (m, 3H), (m, 14H), 8.8 (s, 4H), 11.4 (d, 2H). **IR (KBr),  $\nu$ ,  $\text{cm}^{-1}$**  = 3318, 2928, 1838, 1738, 1688, 1622, 1604, 1582, 1497, 1467, 1389, 1351, 1341, 1282, 1243, 1206, 1025. **MS (MALDI-TOF, DHB matrix):  $m/z$**  Calcd for  $\text{C}_{60}\text{H}_{70}\text{N}_4\text{O}_7$ : 959.22, found: 1066.22  $[\text{M}+\text{Ag}]^+$ .

### Fluorescence quantum yield

Fluorescence quantum yield was calculated using the equation,

$$Q_S = Q_R \frac{A_S I_R n_S^2}{A_R I_S n_R^2} \quad (1)$$

Where, Q: quantum yield, I: integrated area of fluorescence spectra, A: absorbance, and n: refractive index. S and R represent solvent and reference respectively. Quinine sulfate in 0.05 N  $\text{H}_2\text{SO}_4$  was used as standard. [1]

## Kinetics of self-assembly

In an isodesmic mechanism, the addition of each monomer is governed by a single equilibrium constant ( $K_e$ ). A smooth sigmoidal curve, without any sharp slope, is indicative of an isodesmic self-assembly mechanism. [2]

The following equations are used for calculating the degree of aggregation ( $\alpha_{agg}$ ), thermodynamic parameters ( $\Delta H$ ,  $\Delta S$ , and  $\Delta G$ ), and degree of polymerization ( $DP_N$ ).

$$\alpha_{agg} = \frac{A_{con} - A_{mon}}{A_{agg} - A_{mon}} \quad (2)$$

where,  $A_{con}$ ,  $A_{mon}$ ,  $A_{agg}$  are the absorbance at a particular concentration, absorbance at monomer state, and absorbance at aggregated state, respectively.

The kinetics of aggregation in **NDI-DOD-I** was studied by plotting absorbance at a particular wavelength against temperature. From the absorbance,  $\alpha_{agg}$  was calculated (using equation 2) and fitted with a sigmoid curve fitting. From the nature of the plot, the self-assembly of these molecules is assumed to follow an isodesmic mechanism

The temperature-dependent data ( $\alpha_{agg}$  vs temperature plot) was fitted to the isodesmic model using the Boltzman equation,

$$\alpha_{agg} = \frac{1}{1 + e^{\left[\frac{T - T_m}{T^*}\right]}} \quad (3)$$

where,  $T_m$  is the melting temperature ( $T_m$  at  $\alpha_{agg} = 0.5$ ) and  $T^*$  is the characteristic temperature that is related to the slope of the function at the melting temperature.

$$T^* = \frac{-RT_m^2}{0.908\Delta H} \quad (4)$$

The degree of aggregation  $\alpha_{agg}$  as a function of temperature,  $T$  is given by,

$$\alpha_{agg} \cong \frac{1}{1 + e \left[ -0.908 \Delta H \frac{T - T_m}{RT_m^2} \right]} \quad (5)$$

From the degree of aggregation, the number-averaged degree of polymerization,  $DP_N$  can be calculated directly, via:

$$DP_N = \frac{1}{\sqrt{1 - \alpha_{agg}}} \quad (6)$$

The  $DP_N$  can then be related to the total concentration of molecules  $C_T$ , and the association constant  $K$ , via:

$$DP_N = \frac{1}{2} + \frac{1}{2} \sqrt{4KC_T + 1} \quad (7)$$

### Gelation studies

The gelator (**NDI-DOD-I**) was dissolved in 0.1 mL of  $\text{CHCl}_3$  followed by the addition of 0.9 mL of MCH. The solvent mixture was heated up to 60 °C and allowed to cool to room temperature to obtain organogel of NDI. The critical gelation concentration for the gelator has been investigated in the  $\text{CHCl}_3$ /MCH mixture and the value of CGC was 5 mg/mL for **NDI-DOD-I**. All the absorption and emission studies of the gel were performed at CGC value.

### Reference

1. M. Brouwer, Standards for photoluminescence quantum yield measurements in solution (IUPAC Technical Report) *Pure Appl. Chem.*, 2011, **83**, 12, 2213–2228.
2. N. Ponnuswamy, G. D. Pantoş, M. M. J. Smulders, J.K. M. Sanders, Thermodynamics of Supramolecular Naphthalenediimide Nanotube Formation: The Influence of Solvents, Side Chains, and Guest Templates, *J. Am. Chem. Soc.* 2012, **134**, 1, 566-573.

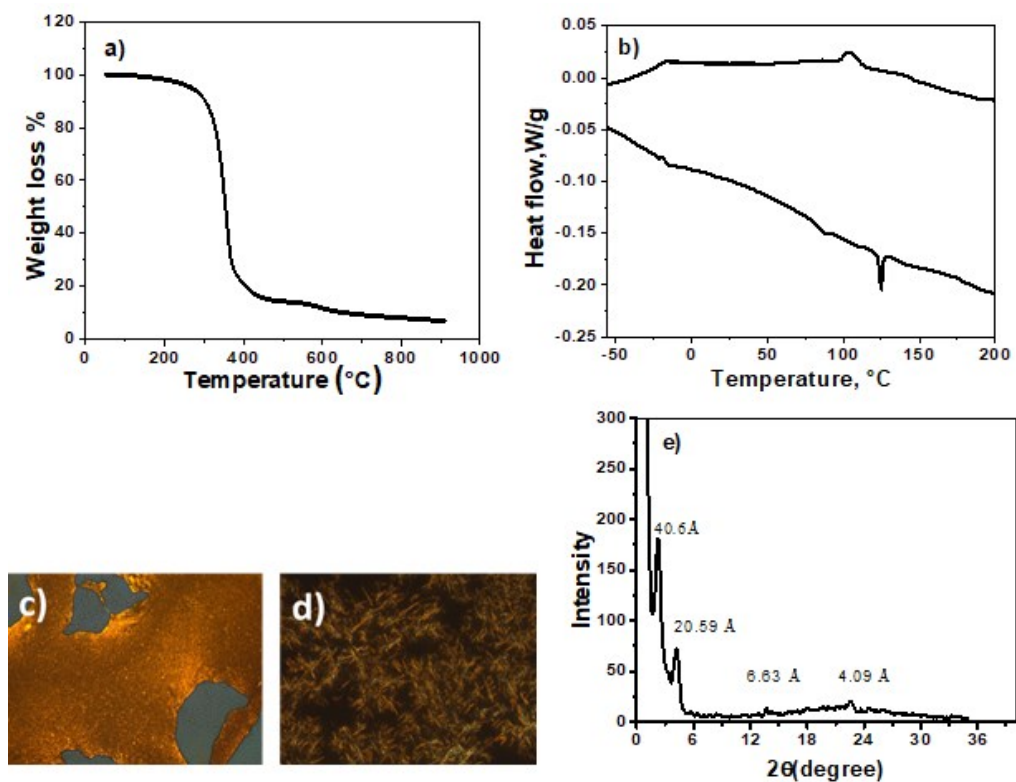


Figure S1: a) TGA, b) DSC thermogram of NDI-DOD-I. Optical microscopy image (OPM) at c) 212 °C (heating, form an isotropic liquid, 10x magnification), d) 44 °C (cooling, crystallizes, 50x magnification), and e) P-XRD pattern of NDI-DOD-I.

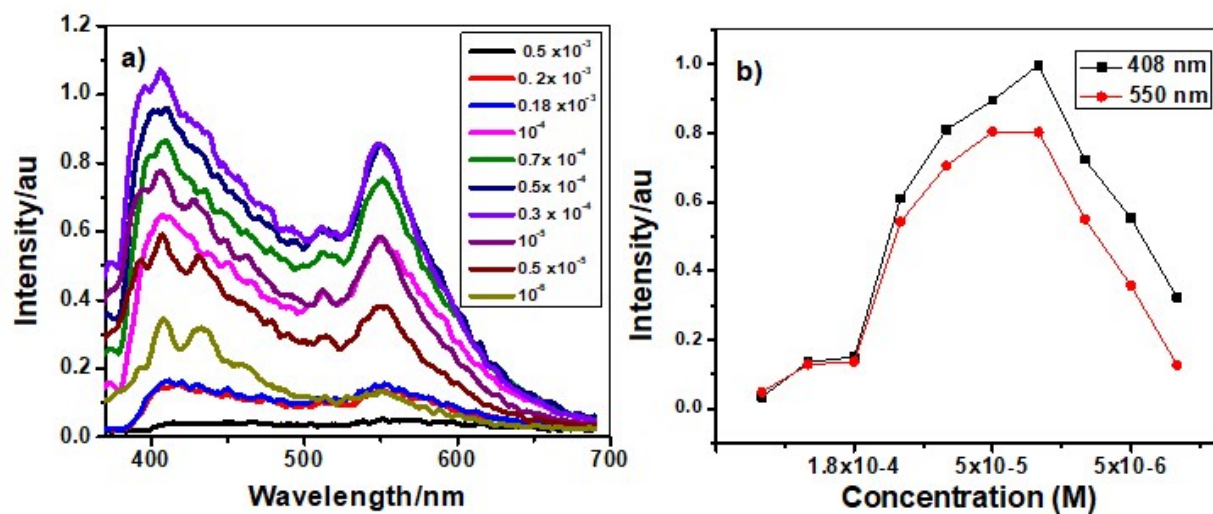


Figure S2: a) Emission spectra of **NDI-DOD-I** in  $\text{CHCl}_3$  by varying the concentration from  $0.5 \times 10^{-3} \text{ M}$  -  $10^{-6} \text{ M}$  and b) plot showing the variation of emission intensity at 404 nm (monomer) and 550 nm (excimer) with different concentration.

Table 1: Absorption and emission peaks of **NDI-DOD-I** in different solvents ( $10^{-5} \text{ M}$ ). Quantum yield values of **NDI-DOD-I** in different solvents using quinine sulphate ( $q_y = 0.54$ ) in 0.05 N  $\text{H}_2\text{SO}_4$  (error  $\pm 5\%$ )

Solvent	$\lambda_{\text{max}}$	$\lambda_{\text{em,max}}$	QY( $\phi_f$ )
DMSO	300, 337, 356, 376	389, 547	0.025
THF	297, 336, 356, 376	406, 527	0.03
DCM	306, 336, 357, 377	393, 553	0.012
$\text{CHCl}_3$	306, 337, 357, 377	410, 548	0.0121
Toluene	305, 335, 360, 384	390, 550	0.011

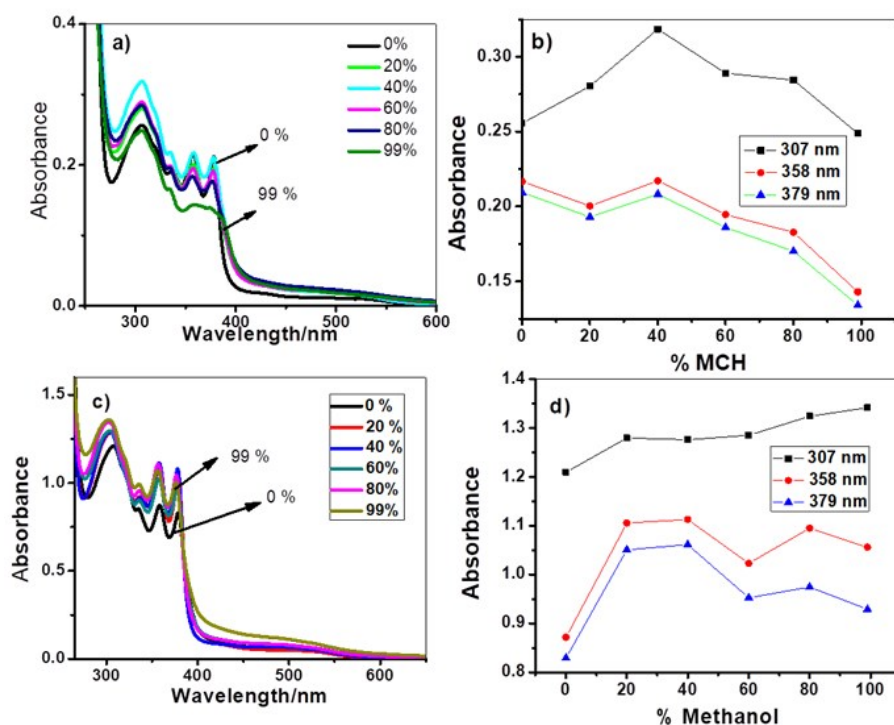


Figure S3: a) Absorption spectra after the addition of different % MCH to a  $10^{-5}$  M solution of **NDI-DOD-I**, b) absorption at a particular wavelength plotted against the % MCH. c) Absorption spectra after the addition of different % methanol to a  $2 \times 10^{-5}$  M solution of **NDI-DOD-I**, and d) absorption at a particular wavelength plotted against the % methanol.

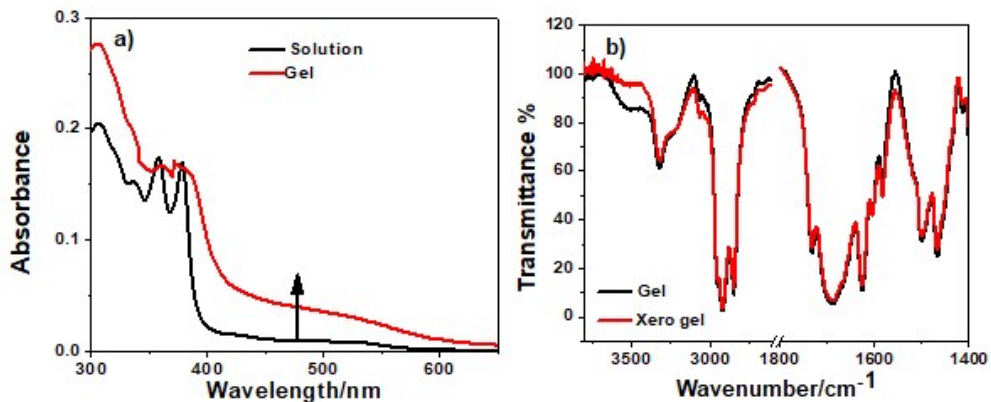


Figure S4: a) Absorption spectra of **NDI-DOD-I** in  $\text{CHCl}_3$  ( $10^{-5}$  M) and gel and b) FT-IR spectra of gel and xero gel of **NDI-DOD-I**.

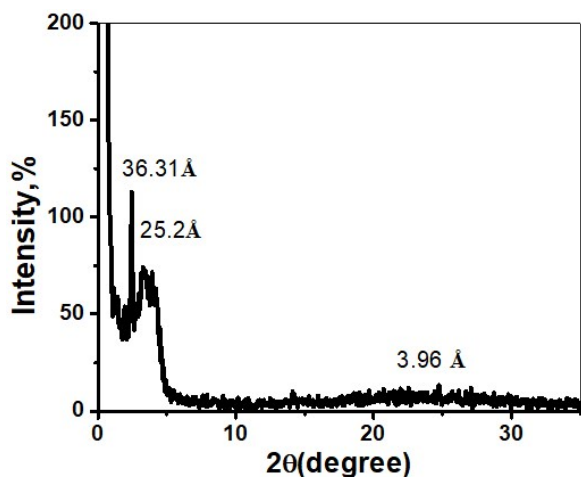


Figure S5: P-XRD pattern of the xerogel.

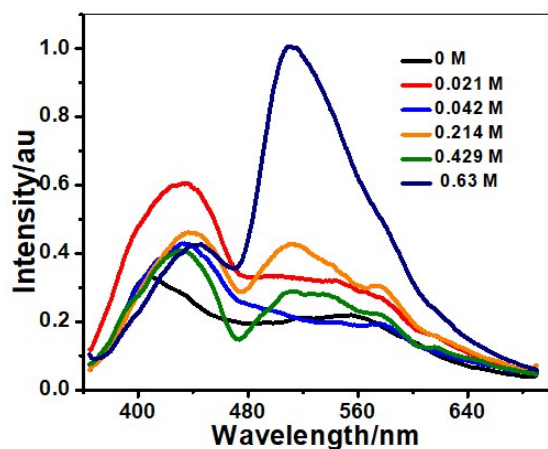


Figure S6: Emission spectra and **NDI-DOD-I** in DMSO ( $5 \times 10^{-5}$  M) after the addition of different molar equivalents of HY (0-0.63 M).

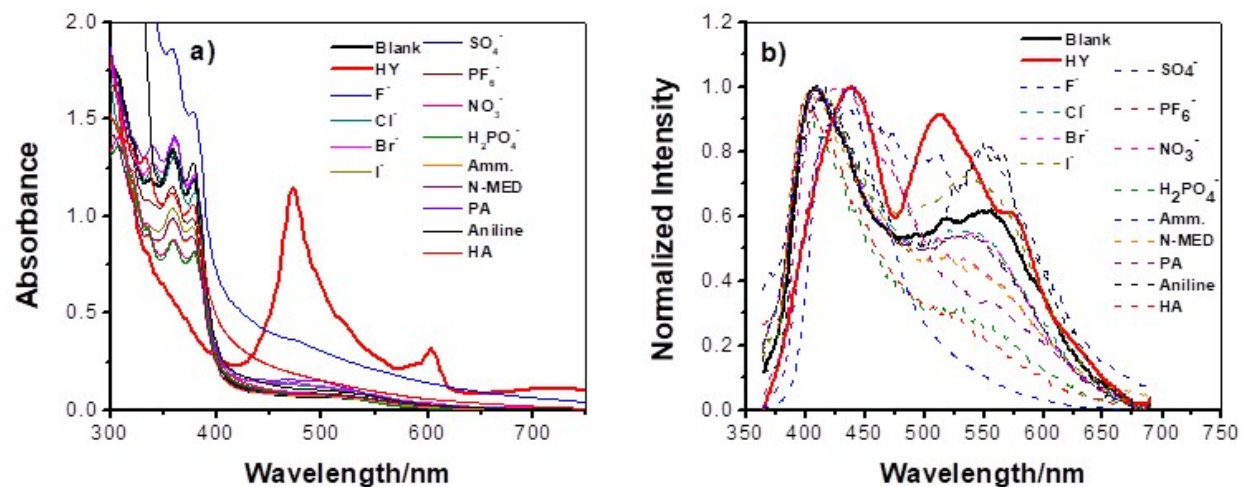


Figure S7: a) Absorption and b) emission spectra of **NDI-DOD-I** in DMSO ( $5 \times 10^{-5}$  M) after the addition of 40 mM concentration of different anions and amine compounds [Amm (ammonia), N-MED (N-methyl ethylenediamine), PA (propylamine), aniline, HA (hydroxylamine)].

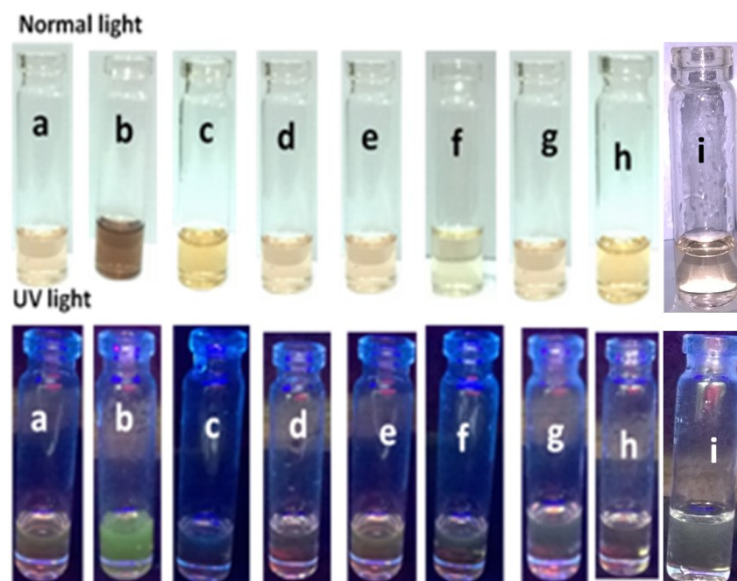


Figure S8: Photographs of **NDI-DOD-I** in DMSO ( $5 \times 10^{-5}$  M) after addition of 40 mM concentration of a) blank, b) HY, c)  $F^-$ , d) other anions e) ammonia, f) N-methyl ethylenediamine, g) propylamine and h) aniline and i) hydroxylamine (anion addition shows almost similar response hence only one representative example is shown).

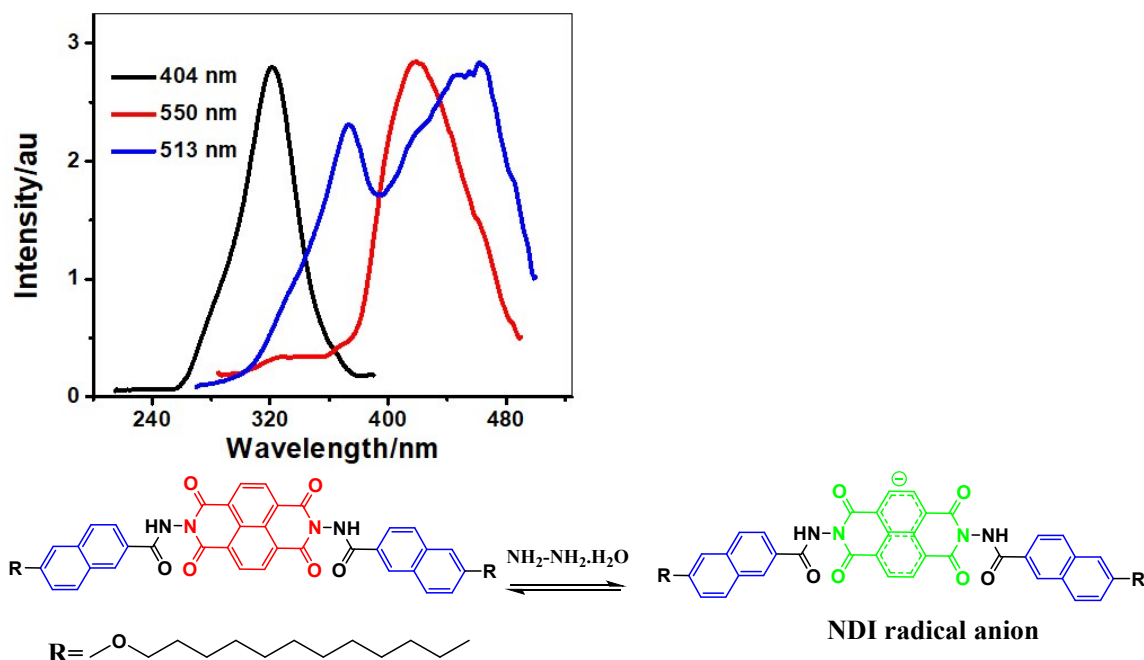


Figure S9: (Above) Excitation spectra of the **NDI-DOD-I** in DMSO ( $5 \times 10^{-5}$  M), before reduction at 404 nm (monomer, excited between 217- 390 nm) 550 nm (excimer, excited between 260-500 nm), and after the reduction at 513 nm (excited between 271- 498 nm). (Below) A schematic representation of NDI radical anion ( $NDI^-$ ) formation after the addition of HY.

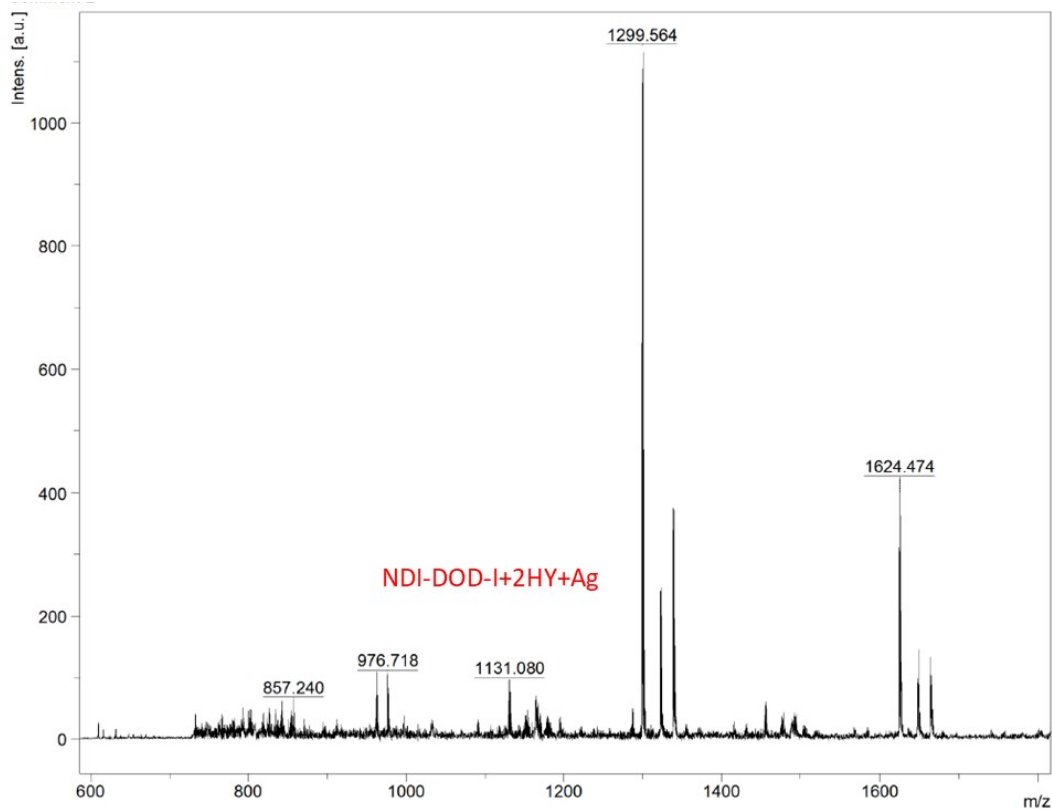


Figure S10: MALDI of **NDI-DOD-I-HY** complex in DHB matrix ( $m/z=1131.080.36$ , **NDI-DOD-I+2HY+Ag**).

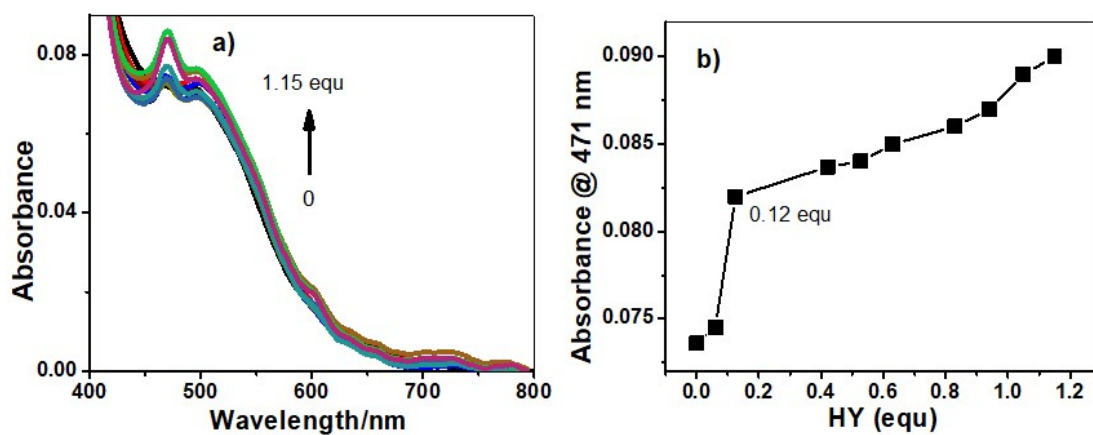


Figure S11: a) Absorption spectra of **NDI-DOD-I** in DMSO at  $7.4 \times 10^{-5}$  M with the addition of 0 - 1.15 equ of HY and b) plot of absorbance at 471 nm against the number of equivalents of HY.

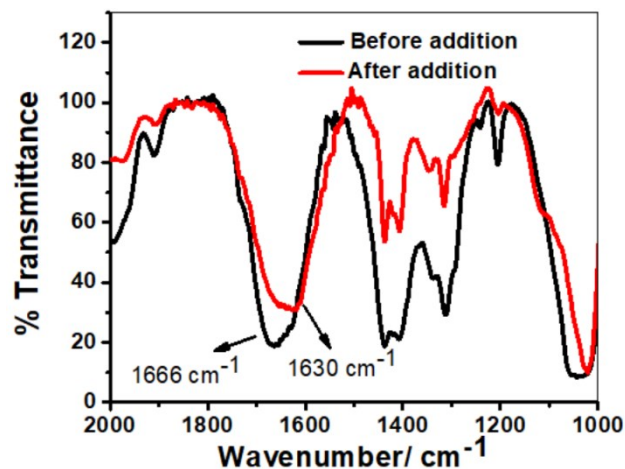


Figure S12: FT-IR spectra of **NDI-DOD-I** before and after the addition of HY (10  $\mu$ L, 0.13 M) in DMSO ( $10^{-4}$  M).

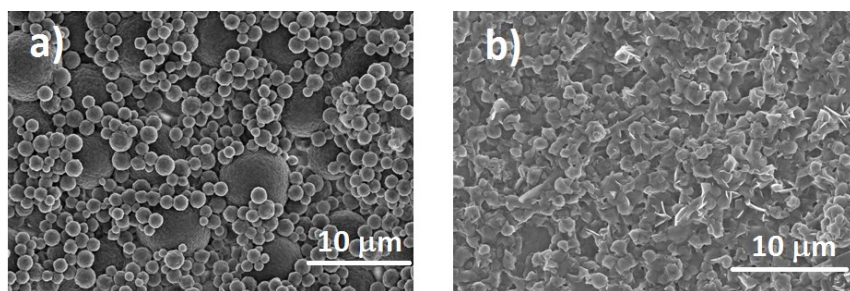


Figure S13: SEM images of **NDI-DOD-I** in DMSO ( $10^{-4}$  M) a) before and b) after the addition of HY (10  $\mu$  L, 0.13 M).

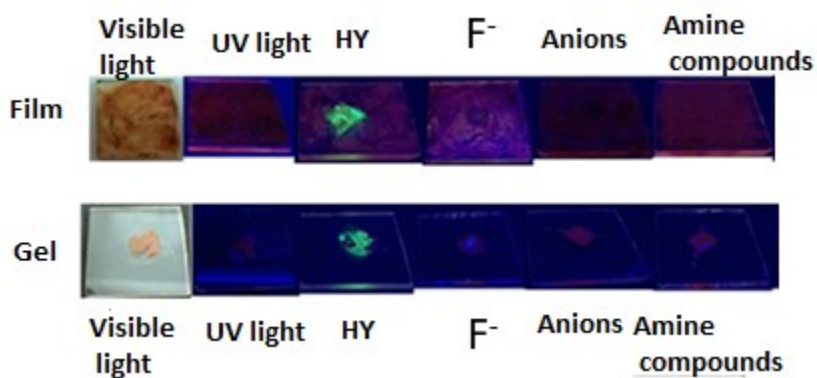


Figure S14: Photographs of **NDI-DOD-I** in the film (drop-casted a  $10^{-3}$  M solution of **NDI-DOD-I** in DMSO and dried in a desiccator) and gel after the addition of 10  $\mu$ L of 0.13 M different analytes (The photographs shown for amines and other anion additions are representative images which shows no radical anion formation).

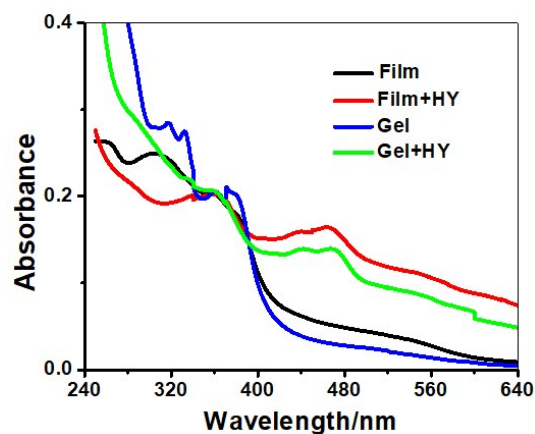


Figure S15: Absorption spectra of **NDI-DOD-I** film and gel before and after the addition of 10  $\mu\text{L}$  of 0.13 M HY.

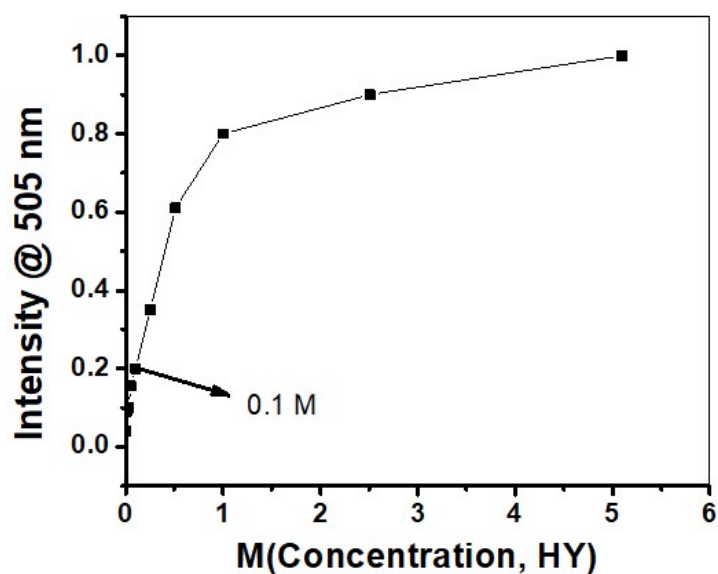


Figure S16: Detection limit calculation using **NDI-DOD-I** gel. (A 1 mg,  $1.05 \times 10^{-6}$  moles of the gel was pasted over the quartz plate over an area of  $1 \text{ cm}^2$  and different equivalents of  $10 \mu\text{L}$  of HY solution were added and monitored the intensity at emission maximum (505 nm)).

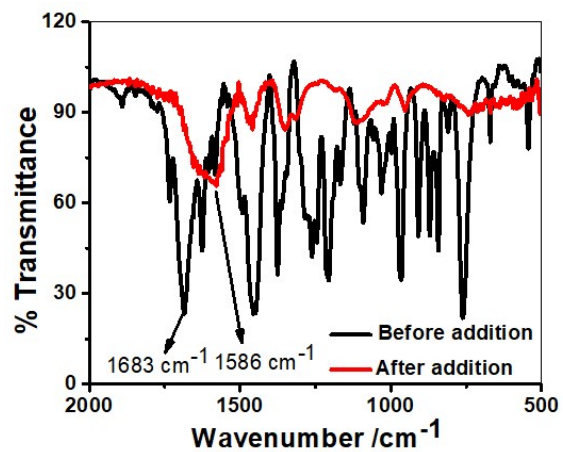
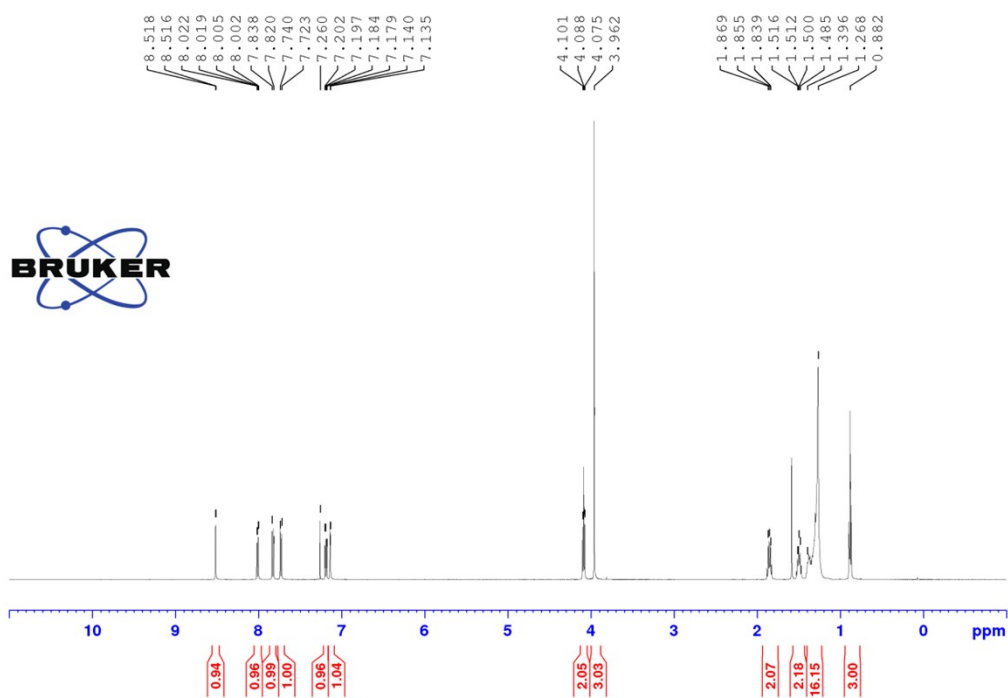


Figure S17: FT-IR spectra of NDI-DOD-I gel pasted over the KBr pellet before and after the reduction using a 10  $\mu\text{L}$  of 0.13 M HY.



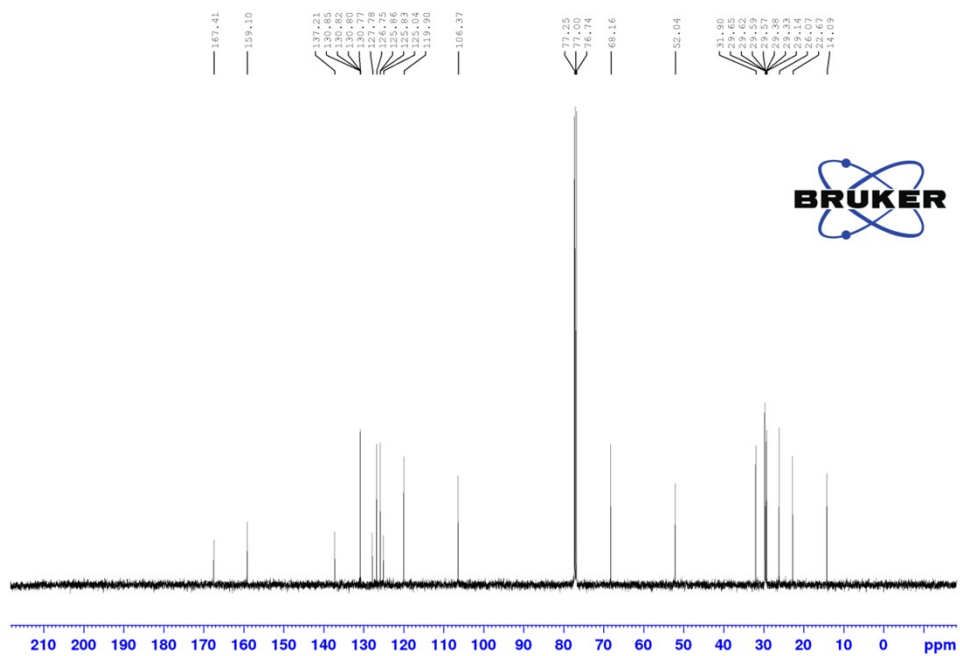
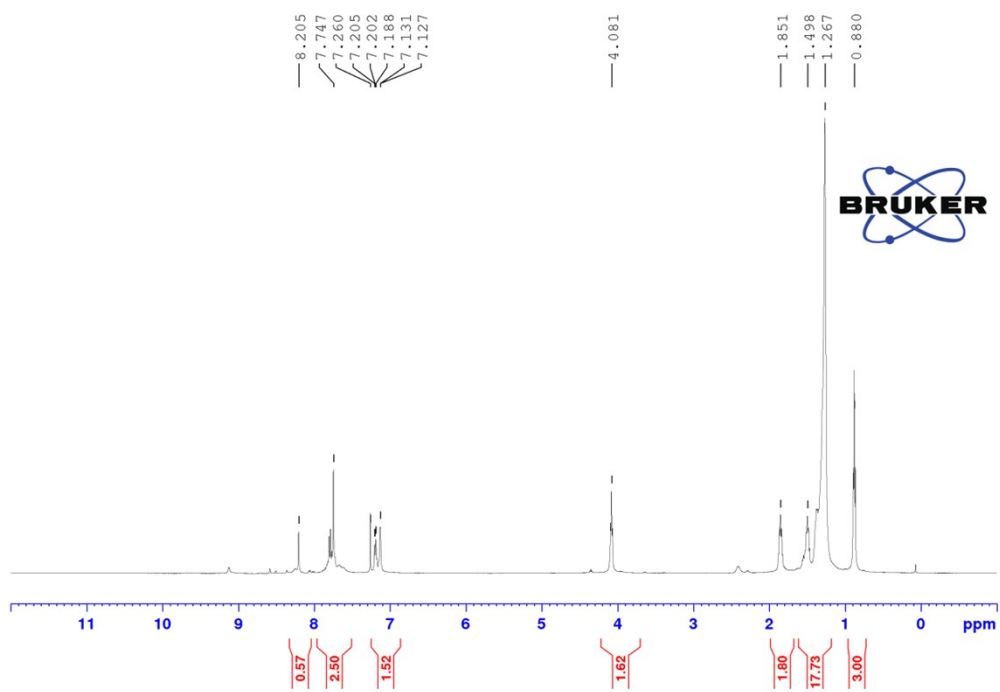


Figure S18:  $^1\text{H}$  and  $^{13}\text{C}$  -NMR spectra of NAPH-EST in  $\text{CDCl}_3$ .



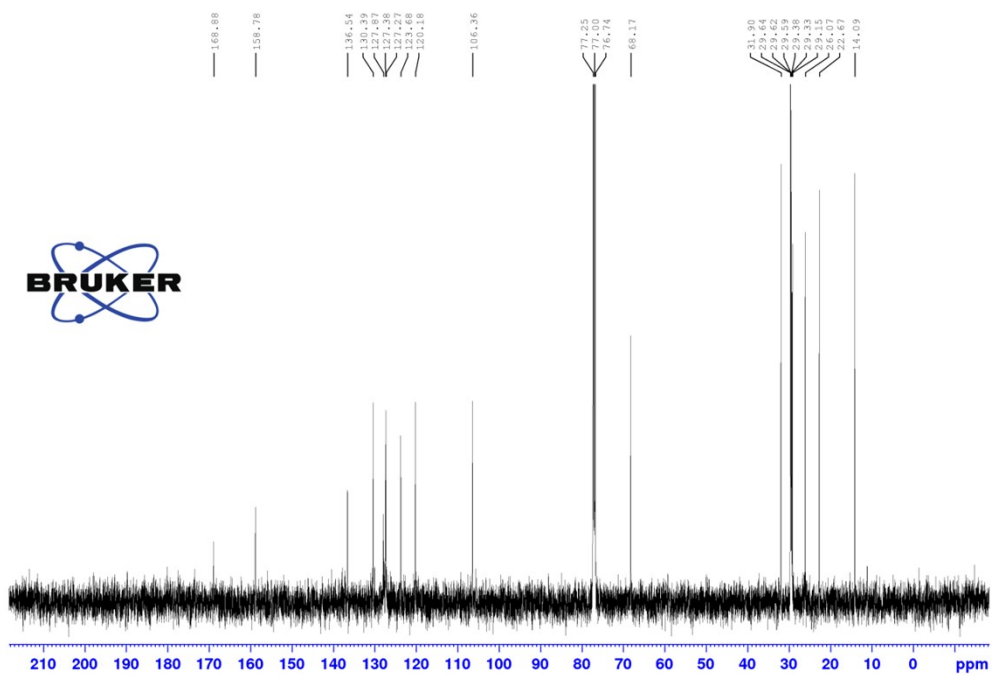


Figure S19:  $^1\text{H}$  and  $^{13}\text{C}$ -NMR spectra of **NAPH-HY** in  $\text{CDCl}_3$ .

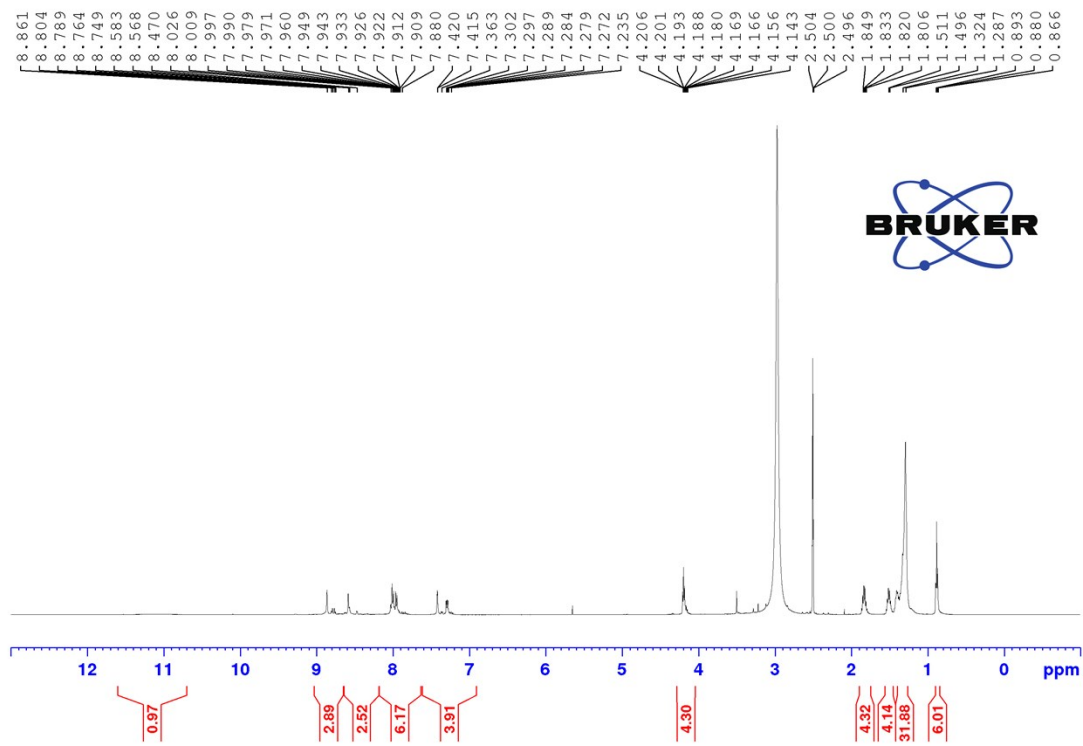


Figure S20:  $^1\text{H}$ -NMR spectra of **NDI-DOD-I** in  $\text{DMSO-d}_6$  at  $120\text{ }^\circ\text{C}$ .

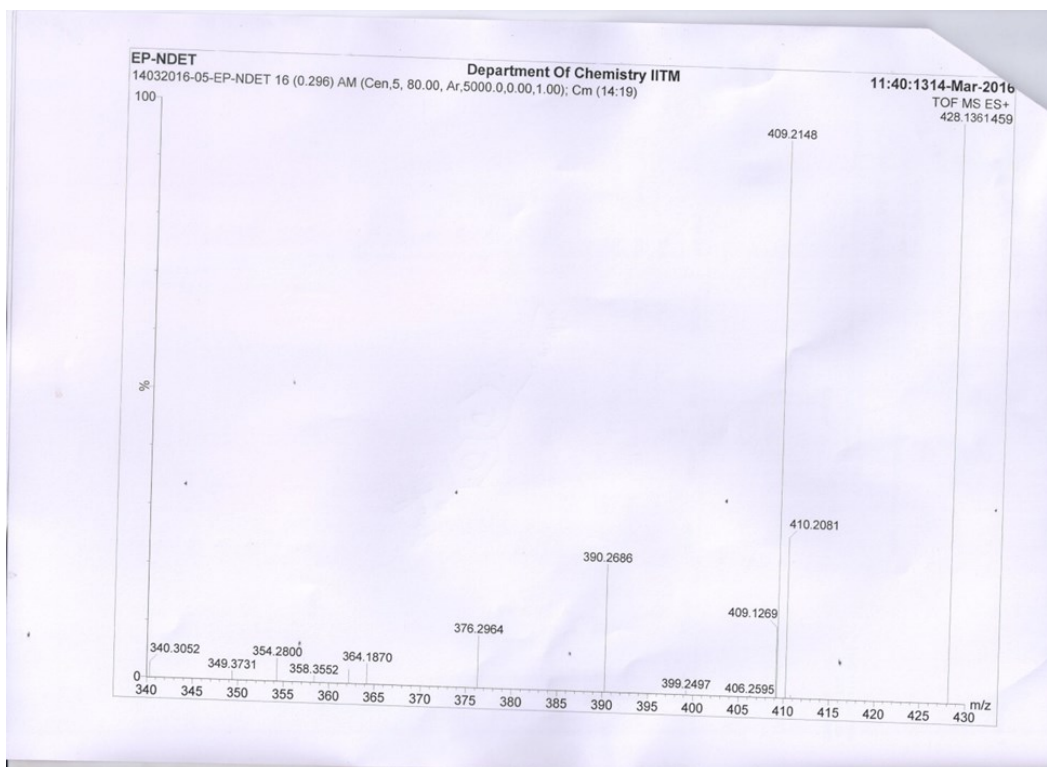


Figure 21: Mass spectrum of **NAPH-EST** (M+K 409.2148).

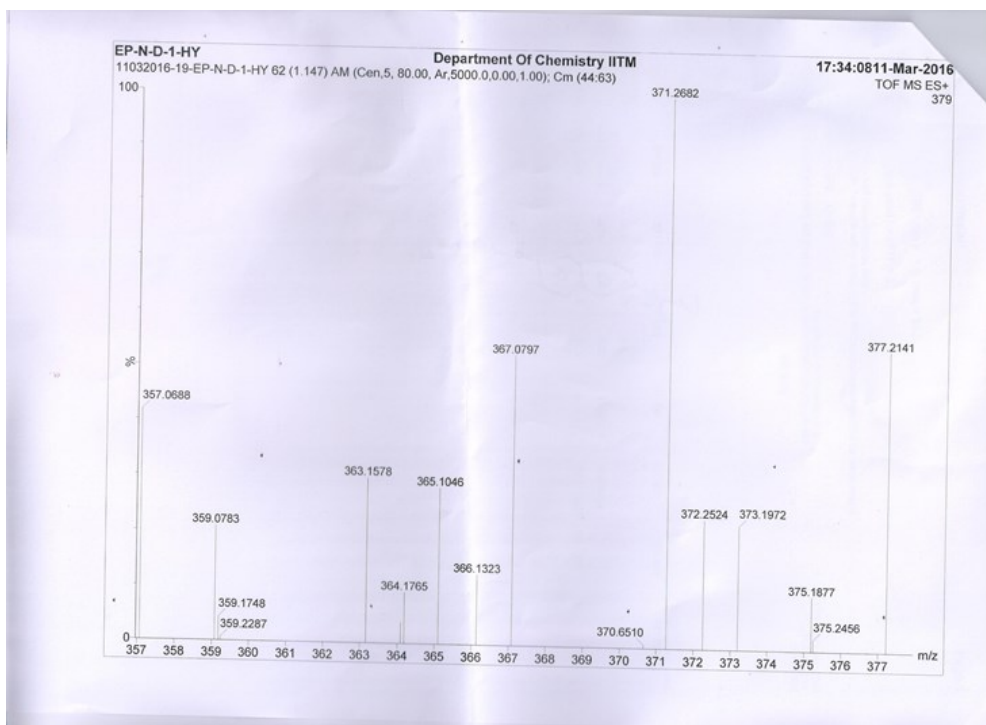


Figure 22: Mass spectrum of **NAPH-HY** (M+H 371.2682).

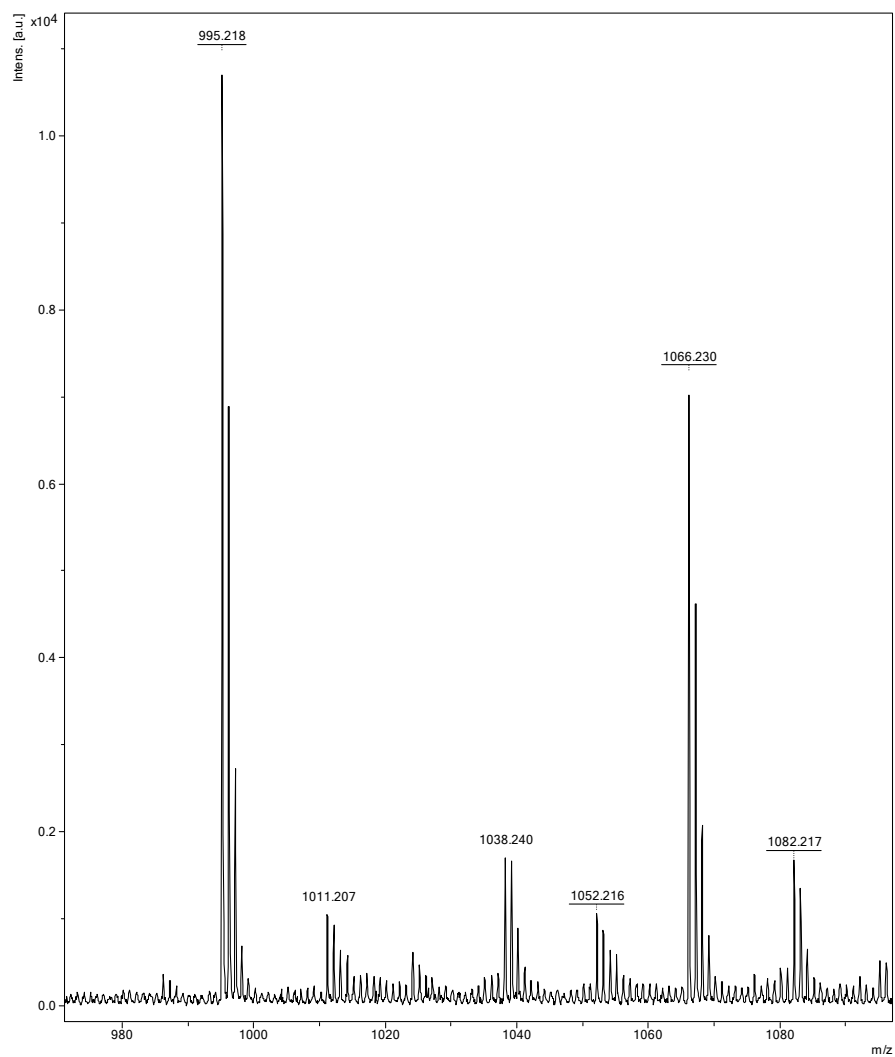


Figure S23: MALDI of **NDI-DOD-I** in the DHB matrix ( $M+Na$  995.210,  $M+K$  1011.207).